

# UC Davis

## UC Davis Previously Published Works

### Title

Aptasensor with Expanded Nucleotide Using DNA Nanotetrahedra for Electrochemical Detection of Cancerous Exosomes

### Permalink

<https://escholarship.org/uc/item/58q896j1>

### Journal

ACS Nano, 11(4)

### ISSN

1936-0851

### Authors

Wang, Sai  
Zhang, Liqin  
Wan, Shuo  
[et al.](#)

### Publication Date

2017-04-25

### DOI

10.1021/acsnano.7b00373

Peer reviewed



Published in final edited form as:

ACS Nano. 2017 April 25; 11(4): 3943–3949. doi:10.1021/acsnano.7b00373.

## Aptasensor with Expanded Nucleotide Using DNA Nanotetrahedra for Electrochemical Detection of Cancerous Exosomes

Sai Wang<sup>†,§,⊥</sup>, Liqin Zhang<sup>†,§,⊥,ID</sup>, Shuo Wan<sup>§</sup>, Sena Cansiz<sup>§</sup>, Yuan Liu<sup>†,§</sup>, Ren Cai<sup>§</sup>, Cheng-Yi Hong<sup>§</sup>, I-Ting Teng<sup>§</sup>, Muling Shi<sup>†,§</sup>, Yuan Wu<sup>†,§</sup>, Yiyang Dong<sup>\*,†</sup>, and Weihong Tan<sup>\*,†,§,ID</sup>

<sup>†</sup>Molecular Science and Biomedicine Laboratory, State Key Laboratory of Chemo/Biosensing and Chemometrics, College of Chemistry and Chemical Engineering, College of Biology, Collaborative Innovation Center for Chemistry and Molecular Medicine, Hunan University, Changsha 410082, China

<sup>‡</sup>Beijing Key Laboratory of Bioprocess, College of Life Science and Technology, Beijing University of Chemical Technology, Beijing 100029, China

<sup>§</sup>Department of Chemistry and Department of Physiology and Functional Genomics, Center for Research at the Bio/Nano Interface, Health Cancer Center, McKnight Brain Institute, UF Genetics Institute, University of Florida, Gainesville, Florida 32611-7200, United States

### Abstract

Exosomes are extracellular vesicles (50–100 nm) circulating in biofluids as intercellular signal transmitters. Although the potential of cancerous exosomes as tumor biomarkers is promising, sensitive and rapid detection of exosomes remains challenging. Herein, we combined the strengths of advanced aptamer technology, DNA-based nanostructure, and portable electrochemical device to develop a nanotetrahedron (NTH)-assisted aptasensor for direct capture and detection of hepatocellular exosomes. The oriented immobilization of aptamers significantly improved the accessibility of an artificial nucleobase-containing aptamer to suspended exosomes, and the NTH-assisted aptasensor could detect exosomes with 100-fold higher sensitivity when compared to the single-stranded aptamer-functionalized aptasensor. The present study provides a proof-of-concept for sensitive and efficient quantification of tumor-derived exosomes. We thus expect the NTH-assisted electrochemical aptasensor to become a powerful tool for comprehensive exosome studies.

\*Corresponding Authors. (Y. Dong): yydong@mail.buct.edu.cn. (W. Tan): tan@chem.ufl.edu.

ORCID

Liqin Zhang: 0000-0002-3632-4117

Weihong Tan: 0000-0002-8066-1524

<sup>⊥</sup>S. Wang and L. Zhang contributed equally.

### ASSOCIATED CONTENT

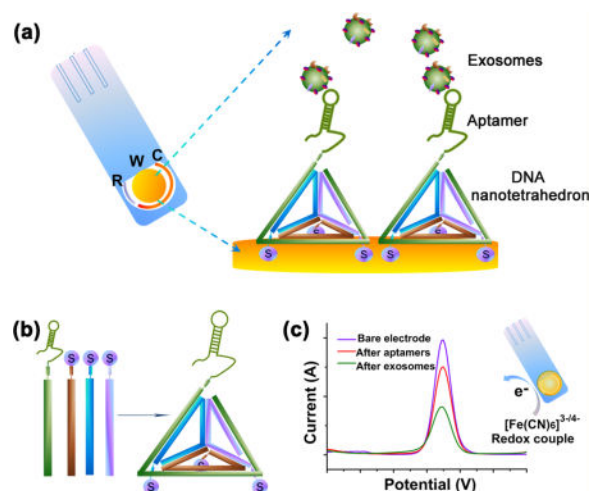
Supporting Information

The Supporting Information is available free of charge on the ACS Publications website at DOI: 10.1021/acsnano.7b00373.

Characterization data of exosomes and DNA, optimization data of SWV, scheme of ss-DNA aptasensor, definition of relative signal, and DNA sequences (PDF)

The authors declare no competing financial interest.

## Graphical Abstract



## Keywords

aptasensor; exosomes; nanotetrahedron; expanded nucleotide; electrochemistry

Exosomes are nanoscale extracellular vesicles (50–100 nm) released from multivesicular bodies through an endolysosomal pathway.<sup>1,2</sup> Exosomes carry abundant macromolecules from their parental cells, including transmembrane and cytosolic proteins, mRNA, DNA, and microRNA,<sup>3–5</sup> thus serving as messengers for mediating intercellular communication.<sup>6</sup> On the basis of their significant role in indicating disease-related, especially cancer-related, alteration of physiological status, exosomes have been recognized as promising biomarkers for early cancer diagnosis, thereby overcoming challenges in cancer detection, such as the expense of invasive screening and low sensitivity.<sup>4,5,7–11</sup>

Despite the numerous publications of qualitative studies, quantification of exosomes remains challenging. One difficulty involves the direct and specific analysis of the nanoscale exosomes. For example, flow cytometry detection is limited by weak light scattering, and particle-tracking methods fail at detection with specificity. Another problem involves the detection of exosomes in low concentration, commonly occurring in the early stage of disease, which requires highly sensitive methods. Moreover, given the tedious steps required to isolate exosomes from body fluids, it is not easy to collect abundant samples for continuous analysis using current methods.<sup>12,13</sup> Meanwhile, techniques capable of analyzing samples in small amounts, such as surface plasmon resonance-based methods,<sup>14,15</sup> involve expensive instrumentation and sophisticated technical skills. There is therefore a growing need for sensitive and reliable methods to probe tumor-derived exosomes rapidly and specifically, yet with modest requirements of sample volumes.

Electrochemical methods, especially aptamer-based biosensors (aptasensors), have drawn particular attention for their applications in cancerous exosome research. Such methods have intrinsic advantages in terms of sensitive recognition, rapid response, excellent portability, modest requirement of sample volumes, and easy signal amplification.<sup>16–20</sup> Compared to

other probes, aptamers generated from *in vitro* selection have many advantages, including high affinity and excellent specificity.<sup>21–25</sup> However, several major limitations have impeded widespread adoption of this method for exosome detection. Currently, for instance, aptamers developed for targeting exosomes are very rare, which, in part, can be attributed to the lack of efficient aptamer selection methods. Moreover, as a consequence of the flexibility of single-stranded DNA, immobilized aptamers on electrodes tend to undergo self-assembled monolayer aggregation or entanglement, which largely impede accessibility of the target exosomes.<sup>26</sup> It is also difficult to control the spatial orientation of single-stranded aptamers with precision.

To overcome these limitations, we herein report an aptasensor incorporating an expanded nucleotide-containing aptamer into a DNA nanotetrahedron (NTH) structure for enhanced electrochemical detection of cancerous exosomes (Scheme 1a). Aptamer LZH8 (Table S1) was generated from a modified *in vitro* selection, termed cell-LIVE, wherein two expanded genetic alphabets (Z and P) were introduced into the initial library for aptamer selection against liver cancer cells.<sup>25</sup> This ATGCZP library serves as a better reservoir to provide increased functionality, as well as increased information density, thereby generating aptamers more efficiently. LZH8, containing one expanded nucleotide along with the regular four nucleotides, showed superior binding selectivity on target hepatocarcinoma cells (HepG2) compared to control noncancerous liver cells (Hu1545), demonstrating satisfactory binding affinity with a dissociation constant of 96 nM. In a screening of aptamers generated from cell-based selection for their binding abilities on exosomes derived from homologous cells, LZH8 exhibited selectivity for HepG2 exosomes over Hu1545 exosomes (another study of our group: Wan, S.; Zhang, L. Q.; Wang, S.; Liu, Y.; Wu, C. C.; Cui, C.; Sun, H.; Shi, M. L.; Jiang, Y.; Li, L.; Qiu, L. P.; Tan, W. H. Molecular Recognition-Based DNA Nanoassemblies on the Surfaces of Nanosized Exosomes, under review).

NTHs, self-assembled from four single-stranded sequences, have been reported to improve specificity and capture efficiency when incorporated into aptasensors for electrochemical detection.<sup>26–28</sup> Briefly, aptamers are built into one of the NTH sequences, while the other three end with thiol groups (Scheme 1b). After immobilization of the bottom pyramidal structure by interactions between the thiols and gold electrode, the individual aptamer strands are distributed at defined nanoscale distances, thereby decreasing the hindrance effect and maintaining spatial orientation for improved biomolecular recognition. In this way, the strengths of advanced aptamer technology and DNA-based NTHs are combined in a rapid and portable aptasensor for the detection of cancerous exosomes.

## RESULTS AND DISCUSSION

We first isolated cancerous exosomes following the previously published protocol.<sup>9</sup> Briefly, the culture medium of HepG2 cells was collected and subjected to a 0.22  $\mu\text{m}$  filter and an ultracentrifuge at 100000g for 2 h. Transmission electron microscopy (TEM) observation was used to validate exosome isolation. As shown in Figure 1a, the diameters of purified vesicles were uniformly distributed at approximately 80 nm, which corresponds to the reported distribution range used to distinguish exosomes from other cell-derived vesicles.<sup>29</sup> Nanoparticle tracking analysis (NTA) results confirmed the size distribution of collected

exosomes (Figure S1). In another validation, hepatocellular exosomes were immobilized on aldehyde latex beads and immunostained by fluorescein isothiocyanate (FITC)-labeled antibodies against a representative surface marker of exosomes, human epithelial cell adhesion molecule (EpCAM).<sup>30</sup> The fluorescence signal was confirmed by flow cytometry (Figure 1b). Similarly, immobilized exosomes also interacted with biotinylated LZH8 aptamer followed by streptavidin-phycoerythrin (SA-PE), and the significant shift of the aptamer-conjugated exosomes compared to the background confirmed the binding ability of LZH8 on HepG2 exosomes (Figure 1c). In addition, immunogold labeling imaged by TEM was further performed to visualize the interaction between aptamers and collected exosomes, using biotinylated LZH8 and streptavidin-coated gold nanoparticles (SA-AuNP). It was observed that the 10 nm gold nanoparticles were attached to the surfaces of exosomes (Figure 1d), but were absent in the control group (no aptamer used, SA-AuNP only, Figure S2), providing solid evidence of the binding ability of aptamer LZH8 to HepG2 exosomes.

After the binding of aptamer LZH8 to HepG2 exosomes was confirmed, we proceeded to the electrochemical analysis. Thiolated aptamer probes were pretreated with tris(2-carboxyethyl)phosphine (TCEP), followed by chemical immobilization on the electrode surface *via* Au–S bonds (Figure S3). The aptamer-functionalized electrodes were then incubated with a suspension of isolated exosomes, and the oriented aptamers captured exosomes directly and specifically. The ferricyanide–ferrocyanide redox couple was used for signal generation by square wave voltammetry (SWV) with the following input parameters: –0.6 to 0.6 V potential range, 0.01 V step potential, 0.05 V amplitude, and 2 Hz frequency (Figure S4). Dramatic signal suppression was observed due to the decreased electrode surface area when covered by the aptamers and exosomes (Scheme 1c).

Single-stranded aptamer LZH8 was first used as the probe in the aptasensor to detect HepG2 hepatocellular exosomes, using HepG2 cells as a positive control. Different aptamer concentrations were tested (with no cells or exosomes) to determine an optimal immobilized concentration. As shown in Figure 2a, current signal differed significantly with aptamer concentration varying from 250 to 2000 nM; 500 nM was chosen, because the immobilized condition caused obvious current change compared with 250 nM ( $P < 0.05$ ) and higher coverage of aptamers (>500 nM) on the electrode could result in limited recognition because of the intermolecular interference among DNA probes. After blocking unreacted Au sites with mercaptoethanol (MCH), electrodes functionalized with LZH8 or a random DNA sequence (negative control) were incubated with HepG2 cells or HepG2 exosomes. As shown in Figure 2b, the redox signal of the LZH8-functionalized electrode (black curves) decreased in the presence of  $10^6$ /mL HepG2 cells, while no significant signal suppression was observed for the random DNA-functionalized electrode (blue curves). Figure 2c shows that signal suppression with the LZH8 electrode decreased as the cell concentration increased. Likewise, detection of exosomes exhibited a similar pattern, showing the reliability of the developed method. These results also confirmed the assumption that hepatocellular exosomes contain molecular information inherited from their parent cells and can therefore serve as potential disease-related biomarkers.

NTHs were then introduced to enhance detection efficiency. The NTH was self-assembled from three TCEP-pretreated 5'-thiolated sequences and one 5'-aptamer-conjugated

sequence (Scheme 1b, Figure S5, Table S1), by simply heating and “snap-cooling”. As shown in Figure 3a, results from 3% agarose gel characterization demonstrated the successful formation of NTHs. The NTHs migrated more slowly than combinations constructed of fewer than four sequences, and the rapid and specific DNA hybridization ensured the high yield of NTH as the only major clear band observed on the gel.

Compared with single-stranded aptamer LZH8, the introduction of NTH significantly improved signal suppression (Figure 3b). The relative electrochemical signal is defined as [(peak current without exosomes– peak current with exosomes)/(peak current without exosomes) × 100%] (Figure 3b). To compare the direct capture efficiency, both single-stranded aptamer-functionalized and tetrahedral aptamer-functionalized electrodes were exposed to a  $10^{13}$ /mL suspension of exosomes. Compared to the single-stranded aptamer, the tetrahedral aptamer led to a 24.1% increase in the relative current signal change, showing superior capture efficiency.

Next, a series of concentrations of hepatocellular exosomes ( $1 \times 10^4$  to  $10^{13}$ /mL) were analyzed in order to further validate this method. Figure 3c presents the comparison of SWV signals obtained with electrodes functionalized with single-stranded aptamer and tetrahedral aptamer. Significance analysis of signal suppressions between different concentrations and  $1 \times 10^4$  /mL was performed using a two-tailed *t* test. Detectable concentration was defined as the concentration from which there is significant difference ( $P < 0.05$ ). Upon replacing single-stranded aptamer with tetrahedral aptamer, the detectable concentration was lowered from  $10^8$  to  $10^6$  exosomes/mL, and the detectable range was also extended (Figure 3c). To further validate the sensitivity of the aptasensors, linear points of the concentration–signal curves in Figure 3c were fitted and the limit of detection (LOD) was defined as the concentration that corresponded to 3 standard deviations below the control ( $1 \times 10^4$ /mL). The LOD of the LZH8-assisted aptasensor was calculated to be  $3.96 \times 10^5$ /mL (Figure 3e), and the LOD of the NTH-assisted aptasensor was calculated to be  $2.09 \times 10^4$ /mL (Figure 3f). The improved sensitivity may have resulted from the mechanical rigidity and structural stability of the pyramidal structure containing three thiol moieties.<sup>31,32</sup> It is also possible that NTHs are anchored on the gold electrodes with highly ordered orientation, thus keeping aptamers at a fixed distance from the electrode surface because of the height of the NTH. Aptamers can therefore fold better to bind with exosomes. In contrast, the immobilized single-stranded aptamers were arrayed in a crowded manner that precluded accessibility because of steric hindrance.

We further tested the selectivity of the NTH-based aptasensor using Hu1545 cell-derived exosomes. The relative suppressions due to the HepG2 cell-derived exosomes are significantly greater than those for the Hu1545 cell-derived exosomes (Figure 3d), demonstrating excellent selectivity for hepatocellular exosome detection. Previously, when using immobilized exosomes at the initial concentration of  $10^{13}$ /mL and fluorescent aptamer staining monitored by flow cytometry, no evidence emerged to suggest that aptamer LZH8 bound noncancerous exosomes (another study of our group: Wan, S.; Zhang, L. Q.; Wang, S.; Liu, Y.; Wu, C. C.; Cui, C.; Sun, H.; Shi, M. L.; Jiang, Y.; Li, L.; Qiu, L. P.; Tan, W. H. Molecular Recognition-Based DNA Nanoassemblies on the Surfaces of Nanosized Exosomes, under review). This indicates that the current aptasensor-based analytical method

is superior in sensitivity, allowing the detection of proteins expressed in lower abundance, which are otherwise untraceable.

The NTH-assisted aptasensor offers advantages in both assay design and practical application. An expanded nucleotide-containing aptamer was applied for detection of cancerous exosomes. The detection range was enhanced as a result of oriented immobilization of aptamers by the introduction of nanotetrahedra, enabling the direct capture and detection of hepatocellular exosomes in a rapid and direct way by an affordable and miniaturized electrochemical system.

Exosomes represent a newly emerging source of biomarkers. Probing this resource requires molecular tools able to recognize such biomarkers in complex biological milieu with high specificity and affinity. The present work demonstrates that aptamers targeting cells can be used to target exosomes, given the homology of their membrane proteins. This recently developed aptamer selection technology with expanded nucleobases strengthened this capability by introducing both functionality and information density, thus delivering aptamers with much higher efficiency.

## CONCLUSIONS

In conclusion, a portable electrochemical aptasensor was developed for rapid and direct detection of hepatocellular exosomes. The present detection method combines the strengths of electrochemical methods, DNA nanostructures, and DNA aptamers with an expanded nucleotide. Compared to the single-stranded aptamer, the tetrahedrally oriented immobilized aptamers significantly improve sensitive electro-chemical performance for capturing exosomes. This method lays the foundation for studying exosome quantification in more complex body fluids. We expect the DNA nanostructure-assisted electrochemical aptasensor to become a powerful tool for comprehensive studies of exosomes and, hence, to accelerate the efficiency of cancer diagnosis.

## MATERIALS AND METHODS

### Materials

All oligonucleotides were synthesized on an ABI3400 DNA/RNA synthesizer (Applied Biosystems, Foster City, CA, USA) with/without thiol labeling. The sequences were then purified by reversed-phase HPLC (ProStar, Varian Walnut Creek, CA, USA). TCEP and MCH were purchased from Sigma-Aldrich (St. Louis, MO, USA). FITC-conjugated anti-human EpCAM antibody and isotype antibody were purchased from BD Biosciences (Sparks, MD, USA). Streptavidin-gold nanoparticles were purchased from Electron Microscopy Sciences (Hatfield, PA, USA). The electrochemical detection was performed on disposable screen-printed electrodes with 4 mm diameter working area (DropSens, Llanera, Spain) connected with a portable potentiostat (Digi-Ivy, Austin, TX, USA), with the input parameters optimized in detail. Binding buffer for cells and exosomes was prepared with Dulbecco's phosphate saline using mM/L  $\text{MgCl}_2$ , 2 g/mL bovine serum albumin (BSA, Fisher Scientific), and 100 mg/L yeast tRNA (Sigma-Aldrich). Washing buffer contained 5 mM/L  $\text{MgCl}_2$  and 2 g/mL BSA. All chemicals were of analytical grade, and all solutions



were prepared with ultrapure water obtained from an ELGA water purification system (Evoqua Water Tech., Lowell, MA, USA).

### Cell Lines

Live cancer cell line HepG2 (ATCC HB-8065) was purchased from American Type Culture Collection (ATCC). Noncancerous liver cell line Hu1545 was a gift from Dr. Chen Liu's lab at Rutgers University and was established by immortalizing primary hepatocytes with lentivirus carrying hTERT (human telomerase reverse transcriptase). The enzyme maintains telomere length at the end of chromosomes and thus enables cells to grow and proliferate. The cell line retains the characteristic protein profile of normal liver cells compared to liver cancer cells. Cells were cultured in high-glucose Dulbecco's modified Eagle's medium (DMEM, Sigma-Aldrich), supplemented with 10% fetal bovine serum (FBS, Gibco, Life Technologies, Carlsbad, CA, USA) and 1% penicillin–streptomycin (PS, Life Technologies), and incubated at 37 °C with 5% CO<sub>2</sub>.

### Exosome Extraction

Exosomes were collected using conventional centrifugation from the supernatant media of HepG2 cells.<sup>9</sup> Cells were harvested in T182 cm<sup>2</sup> flasks in exosome-free FBS-supplemented DMEM until they reached a confluency of 80–90%. Media were collected and centrifuged at 800g for 5 min at 4 °C, and the supernatant was then centrifuged at 2000g for 10 min at 4 °C to discard cellular debris, followed by filtration using a 0.22 μm filter (vacuum-driven filter, 25–229, Genesee Scientific). The filtered media were then ultracentrifuged at 27 000 rpm for 2 h at 4 °C. The pellet was then pipetted, washed with 35 mL of phosphate-buffered saline (PBS), and centrifuged again at 27 000 rpm for 2 h at 4 °C. Finally, the supernatant was discarded, and exosomes were resuspended in 100 μL of PBS. After several collections, the purity and concentration of exosomes were tested and measured using NanoSight (NanoSight Ltd., Malvern, Worcestershire, UK). Stock solutions of 10<sup>13</sup> HepG2-derived exosomes/mL and 10<sup>11</sup> Hu1545v-derived exosomes/mL were obtained, respectively.

### Electrochemical Detection Protocol

Aptamers (LZH8) and monomers for tetrahedron formation were pretreated with 10 mM TCEP at room temperature (RT) for 2 h. Ten microliters of 500 nM single-stranded aptamer LZH8 or 125 nM tetrahedral aptamer LZH8 was immobilized on the surface of electrodes for 3 h at 37 °C, and the unbound aptamers were thoroughly washed away with ultrapure water. After immobilization, the blank sites on the electrodes were then blocked with 1 mM MCH at RT for 2 h. Unbound MCH was thoroughly washed away with ultrapure water. Ten-microliter HepG2 gradient concentrations of cells or exosomes were then incubated with the immobilized aptamers for 30 min at 4 °C, electrodes were washed with ultrapure water, and each step was characterized by SWV. The corresponding concentration of the thiol-labeled random sequence was used as a negative control.

### TEM and Immunogold Labeling for TEM

For TEM observation of pure HepG2 exosomes, the optimal concentration of samples was directly adsorbed on a Formvar/carbon-coated copper grid and dried at room temperature.



For immunogold labeling of samples, an optimal concentration of HepG2 exosomes was placed onto the grids and allowed to be adsorbed. The grids were blocked with 1% BSA/PBS for 1 h, placed on biotin-labeled LZH8 aptamer solution for 1 h at 4 °C, and then rinsed with PBS five times. After washing, the grids were floated on drops of streptavidin-gold nanoparticles for 30 min at 4 °C. Finally, the grids were rinsed with PBS five times and dried at room temperature. As controls, grids were not exposed to LZH8 aptamer. The dried sample was observed on a Hitachi H-7000 NAR transmission electron microscope using a working voltage of 100 kV.

### Immobilization of Exosomes on Latex Beads

Exosomes were attached to 3.8  $\mu\text{m}$  aldehyde/sulfate latex beads (Thermo Fisher Scientific, Waltham, MA USA) by mixing 10  $\mu\text{L}$  of exosomes in a 10  $\mu\text{L}$  volume of beads for 15 min at room temperature with continuous rotation. This suspension was diluted to 1 mL with PBS and rotated for an additional 30 min at room temperature. Reaction was stopped with 100  $\mu\text{L}$  of 1 M glycine and 20% BSA/PBS and rotated for 30 min at room temperature. Then the supernatant stopping solution was removed. The exosome-bound beads were washed in 1 mL of 2% BSA/PBS and centrifuged for 1 min at 14800g, blocked with 10% BSA and 1% salmon sperm DNA (Thermo Fisher Scientific) with rotation at room temperature for 30 min, washed a second time in 2% BSA, centrifuged for 1 min at 14800g, and finally resuspended in 150  $\mu\text{L}$  of 2% BSA/PBS with 5 mM  $\text{Mg}^{2+}$ .

### Binding Test Using Flow Cytometry

Biotin-labeled aptamers (250 nM) were incubated with the immobilized exosomes (diluted in PBS with a ratio of 1:50) in binding buffer at 4 °C for 30 min, followed by centrifugation at 14800g for 1 min with washing buffer. Then, streptavidin/PE (1:400) was incubated with the beads/exosomes, and the beads were washed and suspended in binding buffer (100  $\mu\text{L}$ ). A random sequence was used as control. The fluorescence intensities of PE on the exosomes were determined with an Accuri C6 cytometer (Becton Dickinson Immunocytometry Systems, Sparks, MD, USA). Data were analyzed with the FlowJo software.

### Preparation of Nanotetrahedra

Before the assembly of tetrahedra, the monomers (THa, THb, THc, and THd<sub>1</sub>) were first treated with 10 mM TCEP at room temperature for 2 h to cleave the disulfide linkage. Then, 12.5% N-PAGE gel was used to confirm the reduction result, followed by a Typhoon 9410 variable imager (Figure S5). The nanotetrahedra were assembled from the three thiolated DNA strands of 61 nucleotides (THa, THb, and THc) and one aptamer-containing DNA strand of 122 nucleotides (THd<sub>1</sub>). The DNAs were mixed equivalently in TM buffer (10 mM Tris-HCl, 50 mM  $\text{Mg}^{2+}$ , pH 8.0), heated at 95 °C for 2 min, and then rapidly cooled at 4 °C for 1 min. The random sequence-containing DNA nanotetrahedra were prepared using the same method with THa, THb, THc, and THd<sub>2</sub>. The formation of DNA nanostructures was analyzed using 3% agarose gel electrophoresis in TBE buffer at 100 V for 25 min.

## Supplementary Material

Refer to Web version on PubMed Central for supplementary material.

## Acknowledgments

The authors thank Dr. Kathryn R. Williams for manuscript review. The authors thank Dr. Chen Liu's lab at Rutgers University for providing the Hu1545 cell lines. The authors also thank Dr. Steven Benner's lab at Foundation for Applied Molecular Evolution for providing phosphoramidites for DNA synthesis. The Y.D. laboratory acknowledges support of the NSFC grant (51673012), National Key Research and Development Program of China (2016YFF0203703), and Key Program of Beijing Municipal Science and Technology Commission (D161100002116002). The W.T. laboratory is indebted to the National Institutes of Health (GM079359, GM111386, and CA133086), the National Key Scientific Program of China (2011CB911000), NSFC grants (21505032, 21325520, and 1327009), and China National Instrumentation Program 2011YQ03012412. S.W. acknowledges financial support under the State Scholarship Fund from the China Scholarship Council.

## References

1. Melo SA, Sugimoto H, O'Connell JT, Kato N, Villanueva A, Vidal A, Qiu L, Vitkin E, Perelman LT, Melo CA. Cancer Exosomes Perform Cell-Independent MicroRNA Biogenesis and Promote Tumorigenesis. *Cancer Cell*. 2014; 26:707–721. [PubMed: 25446899]
2. Raposo G, Stoorvogel W. Extracellular Vesicles: Exosomes, Microvesicles, and Friends. *J. Cell Biol.* 2013; 200:373–383. [PubMed: 23420871]
3. Balaj L, Lessard R, Dai L, Cho Y-J, Pomeroy SL, Breakefield XO, Skog J. Tumour Microvesicles Contain Retrotransposon Elements and Amplified Oncogene Sequences. *Nat. Commun.* 2011; 2:180. [PubMed: 21285958]
4. Skog J, Würdinger T, van Rijn S, Meijer DH, Gainche L, Curry WT, Carter BS, Krichevsky AM, Breakefield XO. Glioblastoma Microvesicles Transport RNA and Proteins that Promote Tumour Growth and Provide Diagnostic Biomarkers. *Nat. Cell Biol.* 2008; 10:1470–1476. [PubMed: 19011622]
5. Valadi H, Ekström K, Bossios A, Sjöstrand M, Lee JJ, Lötvall JO. Exosome-Mediated Transfer of MRNAs and MicroRNAs Is a Novel Mechanism of Genetic Exchange between Cells. *Nat. Cell Biol.* 2007; 9:654–659. [PubMed: 17486113]
6. Speicher MR, Pantel K. Tumor Signatures in the Blood. *Nat. Biotechnol.* 2014; 32:441–443. [PubMed: 24811515]
7. Costa-Silva B, Aiello NM, Ocean AJ, Singh S, Zhang H, Thakur BK, Becker A, Hoshino A, Mark MT, Molina H. Pancreatic Cancer Exosomes Initiate Pre-Metastatic Niche Formation in the Liver. *Nat. Cell Biol.* 2015; 17:816–826. [PubMed: 25985394]
8. Hoshino A, Costa-Silva B, Shen T-L, Rodrigues G, Hashimoto A, Mark MT, Molina H, Kohsaka S, Di Giannatale A, Ceder S. Tumour Exosome Integrins Determine Organotropic Metastasis. *Nature*. 2015; 527:329–335. [PubMed: 26524530]
9. Melo SA, Luecke LB, Kahlert C, Fernandez AF, Gammon ST, Kaye J, Lebleu VS, Mittendorf EA, Weitz J, Rahbari N. Glypican-1 Identifies Cancer Exosomes and Detects Early Pancreatic Cancer. *Nature*. 2015; 523:177–182. [PubMed: 26106858]
10. Shao H, Chung J, Lee K, Balaj L, Min C, Carter BS, Hochberg FH, Breakefield XO, Lee H, Weissleder R. Chip-Based Analysis of Exosomal mRNA Mediating Drug Resistance in Glioblastoma. *Nat. Commun.* 2015; 6:6999. [PubMed: 25959588]
11. Zhou YG, Mohamadi RM, Poudineh M, Kermanshah L, Ahmed S, Safaei TS, Stojic J, Nam RK, Sargent EH, Kelley SO. Interrogating Circulating Microsomes and Exosomes using Metal Nanoparticles. *Small*. 2016; 12:727–732. [PubMed: 26707703]
12. Zhou H, Yuen PS, Pisitkun T, Gonzales PA, Yasuda H, Dear JW, Gross P, Knepper MA, Star RA. Collection, Storage, Preservation, and Normalization of Human Urinary Exosomes for Biomarker Discovery. *Kidney. Int.* 2006; 69:1471–1476. [PubMed: 16501490]
13. Ueda K, Ishikawa N, Tatsuguchi A, Saichi N, Fujii R, Nakagawa H. Antibody-Coupled Monolithic Silica Microtips for Highthroughput Molecular Profiling of Circulating Exosomes. *Sci. Rep.* 2014; 4:6232. [PubMed: 25167841]
14. Im H, Shao H, Park YI, Peterson VM, Castro CM, Weissleder R, Lee H. Label-Free Detection and Molecular Profiling of Exosomes with a Nano-Plasmonic Sensor. *Nat. Biotechnol.* 2014; 32:490–495. [PubMed: 24752081]

15. Zhu L, Wang K, Cui J, Liu H, Bu X, Ma H, Wang W, Gong H, Lausted C, Hood L. Label-Free Quantitative Detection of Tumor-derived Exosomes Through Surface Plasmon Resonance Imaging. *Anal. Chem.* 2014; 86:8857–8864. [PubMed: 25090139]
16. Wei F, Patel P, Liao W, Chaudhry K, Zhang L, Arellano-Garcia M, Hu S, Elashoff D, Zhou H, Shukla S. Electrochemical Sensor for Multiplex Biomarkers Detection. *Clin. Cancer. Res.* 2009; 15:4446–4452. [PubMed: 19509137]
17. Hsieh K, Patterson AS, Ferguson BS, Plaxco KW, Soh HT. Rapid, Sensitive, and Quantitative Detection of Pathogenic DNA at the Point of Care Through Microfluidic Electrochemical Quantitative Loop-Mediated Isothermal Amplification. *Angew. Chem.* 2012; 124:4980–4984.
18. Campuzano S, Torrente-Rodríguez RM, López-Hernández E, Conzuelo F, Granados R, Sánchez-Puelles JM, Pingarrón JM. Magnetobiosensors Based on Viral Protein p19 for microRNA Determination in Cancer Cells and Tissues. *Angew. Chem., Int. Ed.* 2014; 53:6168–6171.
19. Das J, Ivanov I, Montermini L, Rak J, Sargent EH, Kelley SO. An Electrochemical Clamp Assay for Direct, Rapid Analysis of Circulating Nucleic Acids in Serum. *Nat. Chem.* 2015; 7:569–575. [PubMed: 26100805]
20. Xia F, White RJ, Zuo X, Patterson A, Xiao Y, Kang D, Gong X, Plaxco KW, Heeger AJ. An Electrochemical Supersandwich Assay for Sensitive and Selective DNA Detection in Complex Matrices. *J. Am. Chem. Soc.* 2010; 132:14346–14348. [PubMed: 20873767]
21. Kim C-H, Lee L-P, Min J-R, Lim M-W, Jeong S-H. An Indirect Competitive Assay-Based Aptasensor for Detection of Oxytetracycline in Milk. *Biosens. Bioelectron.* 2014; 51:426–430. [PubMed: 24011458]
22. Nimjee SM, Rusconi CP, Sullenger BA. Aptamers: An Emerging Class of Therapeutics. *Annu. Rev. Med.* 2005; 56:555–583. [PubMed: 15660527]
23. Tombelli S, Minunni M, Mascini M. Analytical Applications of Aptamers. *Biosens. Bioelectron.* 2005; 20:2424–2434. [PubMed: 15854817]
24. Pultar J, Sauer U, Domnanich P, Preininger C. Aptamer-Antibody On-Chip Sandwich Immunoassay for Detection of CRP in Spiked Serum. *Biosens. Bioelectron.* 2009; 24:1456–1461. [PubMed: 18951012]
25. Zhang L, Yang Z, Sefah K, Bradley KM, Hoshika S, Kim M-J, Kim H-J, Zhu G, Jiménez E, Cansiz S. Evolution of Functional Six-Nucleotide DNA. *J. Am. Chem. Soc.* 2015; 137:6734–6737. [PubMed: 25966323]
26. Lin M, Song P, Zhou G, Zuo X, Aldalbahi A, Lou X, Shi J, Fan C. Electrochemical Detection of Nucleic Acids, Proteins, Small Molecules and Cells using a DNA-Nanostructure-based Universal Biosensing Platform. *Nat. Protoc.* 2016; 11:1244–1263. [PubMed: 27310264]
27. Schlapak R, Danzberger J, Armitage D, Morgan D, Ebner A, Hinterdorfer P, Pollheimer P, Gruber HJ, Schäffler F, Howorka S. Nanoscale DNA Tetrahedra Improve Biomolecular Recognition on Patterned Surfaces. *Small.* 2012; 8:89–97. [PubMed: 22083943]
28. Pei H, Lu N, Wen Y, Song S, Liu Y, Yan H, Fan C. A DNA Nanostructure-based Biomolecular Probe Carrier Platform for Electrochemical Biosensing. *Adv. Mater.* 2010; 22:4754–4758. [PubMed: 20839255]
29. van der Pol E, Böing AN, Harrison P, Sturk A, Nieuwland R. Classification, Functions, and Clinical Relevance of Extracellular Vesicles. *Pharmacol. Rev.* 2012; 64:676–705. [PubMed: 22722893]
30. Runz S, Keller S, Rupp C, Stoeck A, Issa Y, Koensgen D, Mustea A, Sehouli J, Kristiansen G, Altevogt P. Malignant Ascites-Derived Exosomes of Ovarian Carcinoma Patients Contain CD24 and EpCAM. *Gynecol. Oncol.* 2007; 107:563–571. [PubMed: 17900673]
31. Goodman RP, Schaap IA, Tardin CF, Erben CM, Berry RM, Schmidt CF, Turberfield A. Rapid Chiral Assembly of Rigid DNA Building Blocks for Molecular Nanofabrication. *Science.* 2005; 310:1661–1665. [PubMed: 16339440]
32. Mitchell N, Schlapak R, Kastner M, Armitage D, Chrzanowski W, Riemer J, Hinterdorfer P, Ebner A, Howorka S. A DNA Nanostructure for the Functional Assembly of Chemical Groups with Tunable Stoichiometry and Defined Nanoscale Geometry. *Angew. Chem., Int. Ed.* 2009; 48:525–527.

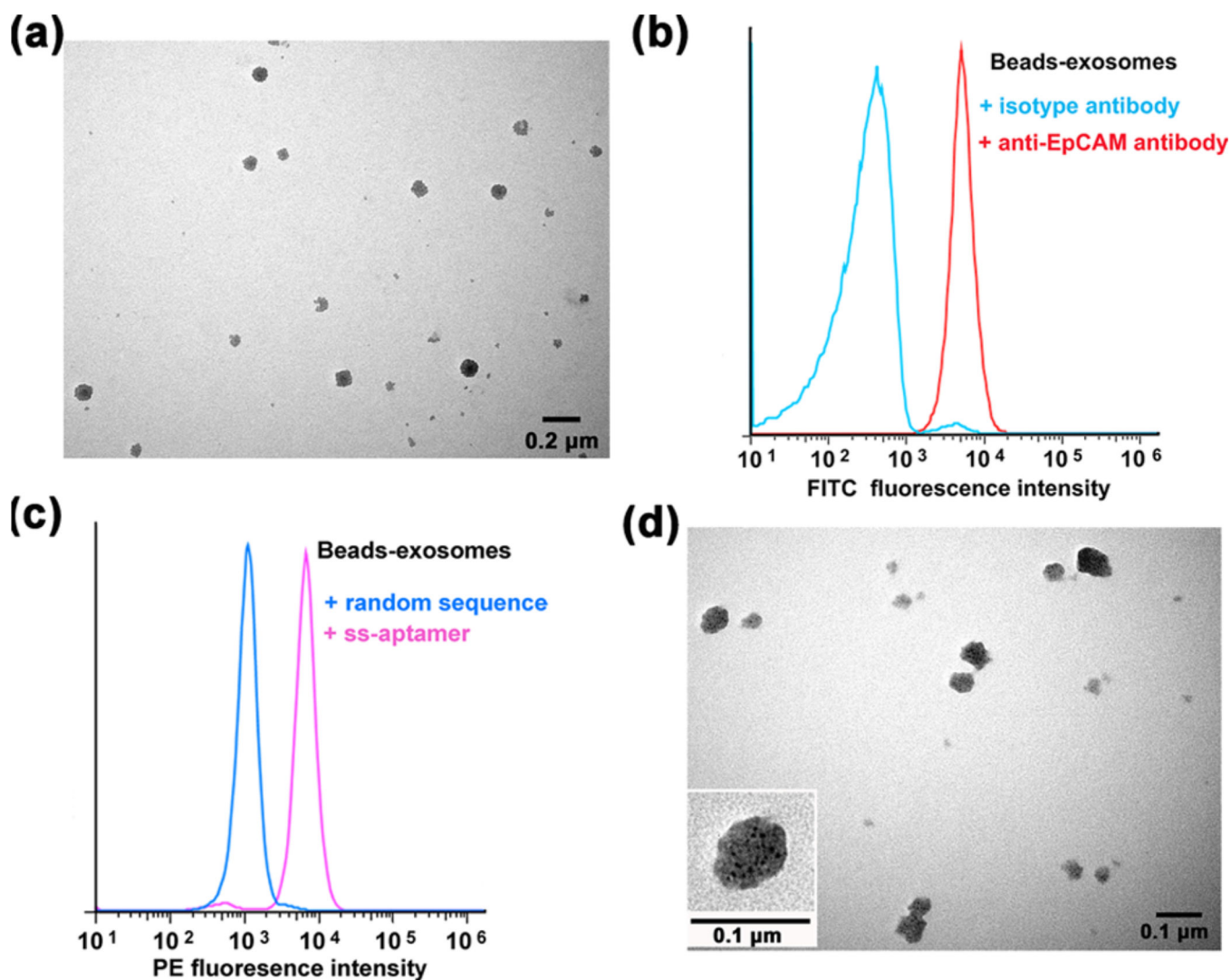


**Figure 1.** Validation of exosome isolation and interaction between aptamer LZH8 and HepG2 exosomes. (a) TEM observation of purified exosomes. (b) Flow cytometry verification of immobilized exosomes using FITC-labeled anti-EpCAM antibody. Isotype antibody indicated the background. (c) Immobilized exosomes recognized by biotinylated aptamer LZH8, stained by SA-PE, and analyzed by flow cytometry. A random sequence indicated the background. (d) Immunogold labeling observed by TEM, showing that SA-AuNP could be attached to the exosome surface *via* conjugation with biotinylated aptamers.

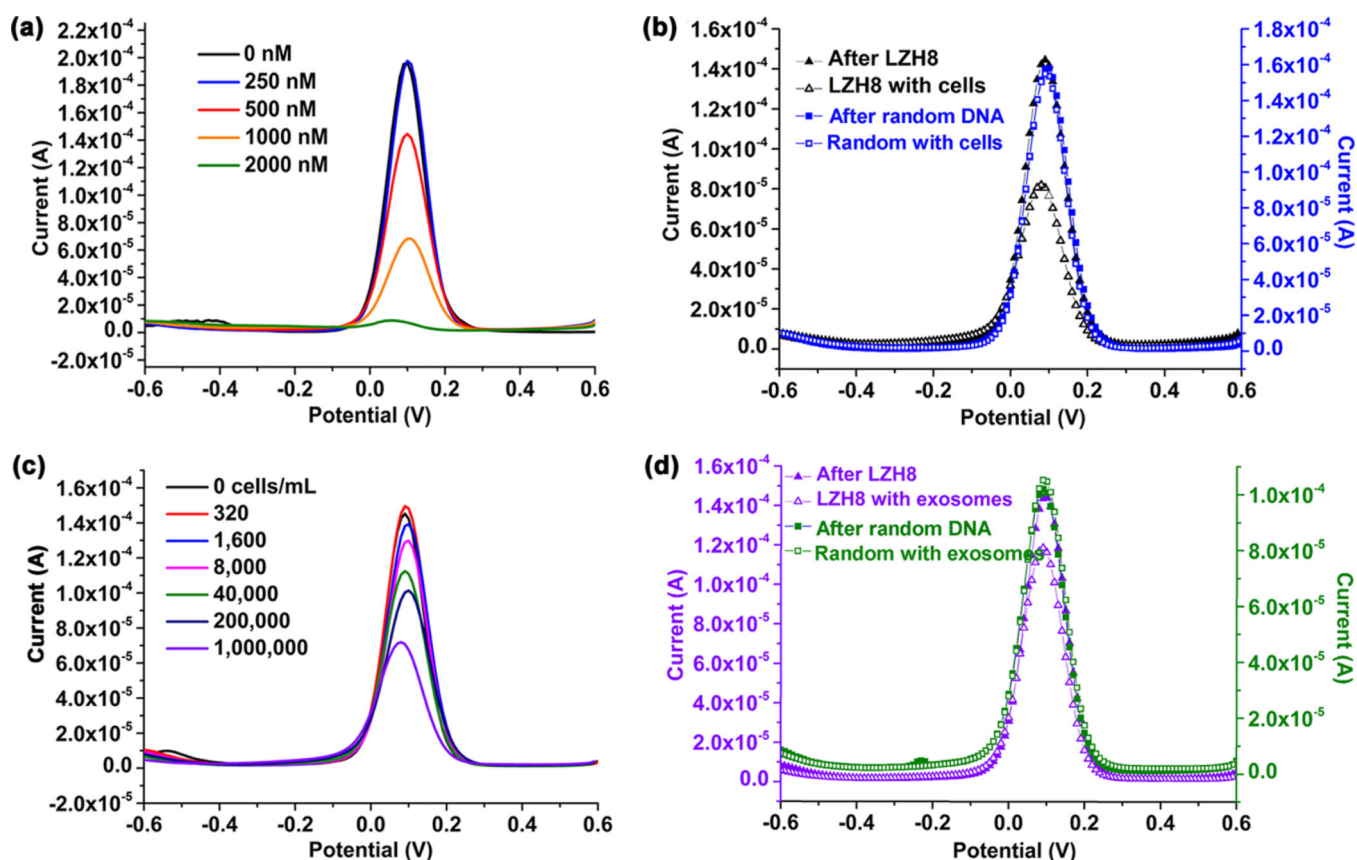


**Figure 2.**

Single-stranded LZH8-functionalized aptasensor for electrochemical detection of hepatocellular cells and exosomes. (a) Optimization of aptamer concentration used for electrode functionalization. (b) Electrochemical signals of the LZH8 or random sequence-functionalized electrodes after incubation with  $10^6$  cells/mL of HepG2 cells. A random sequence was used as negative control to evaluate the nonspecific binding. (c) Concentration-dependent detection of HepG2 cells using LZH8-functionalized aptasensor. The redox signals are directly related to the logarithm of the concentration of HepG2 cells, as detected by LZH8-functionalized electrodes. (d) Electrochemical signals of the LZH8 or random sequence-functionalized electrodes after incubation with  $10^{13}$ /mL of HepG2-derived exosomes. A random sequence was used as a negative control to evaluate the nonspecific binding.



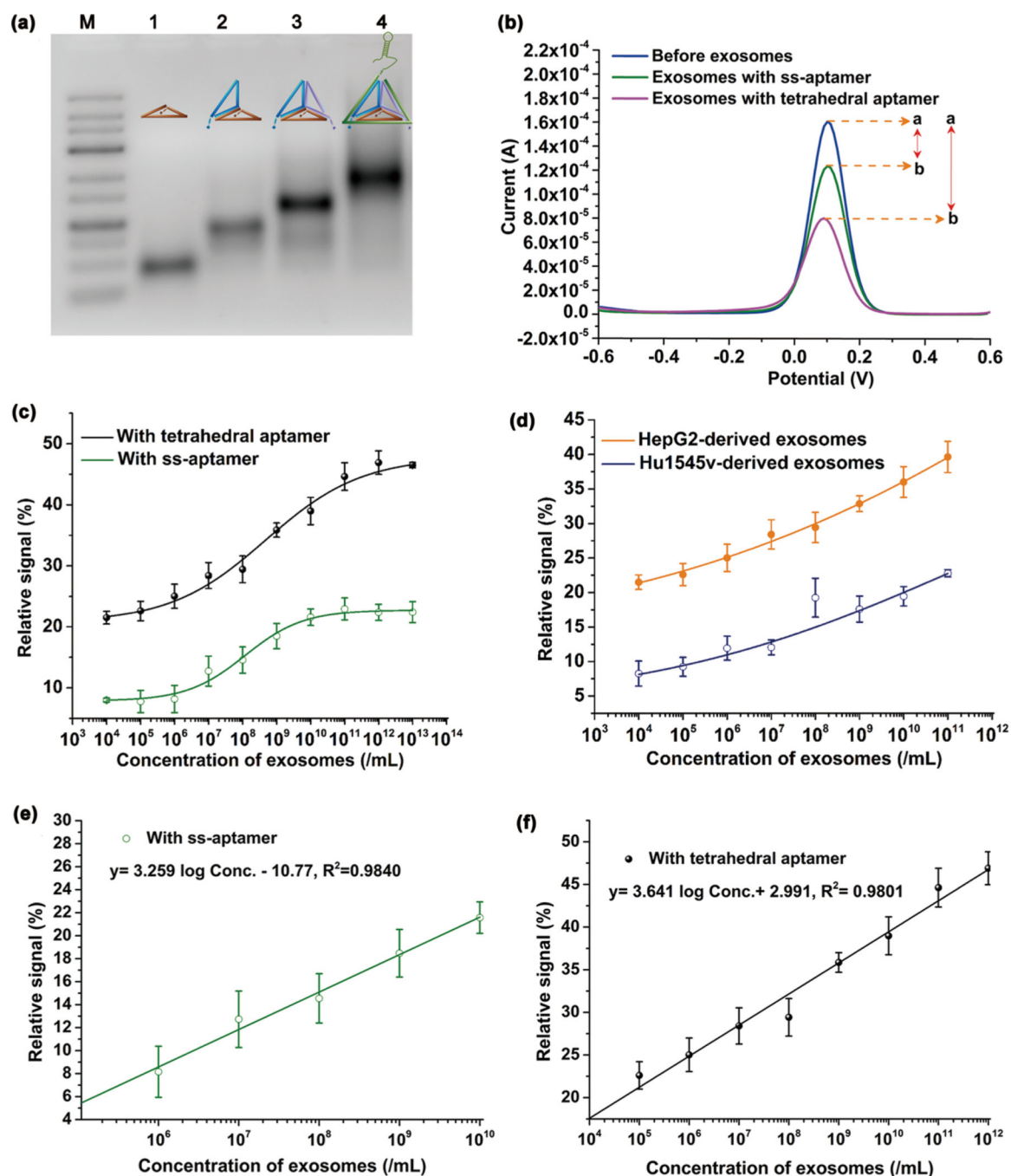
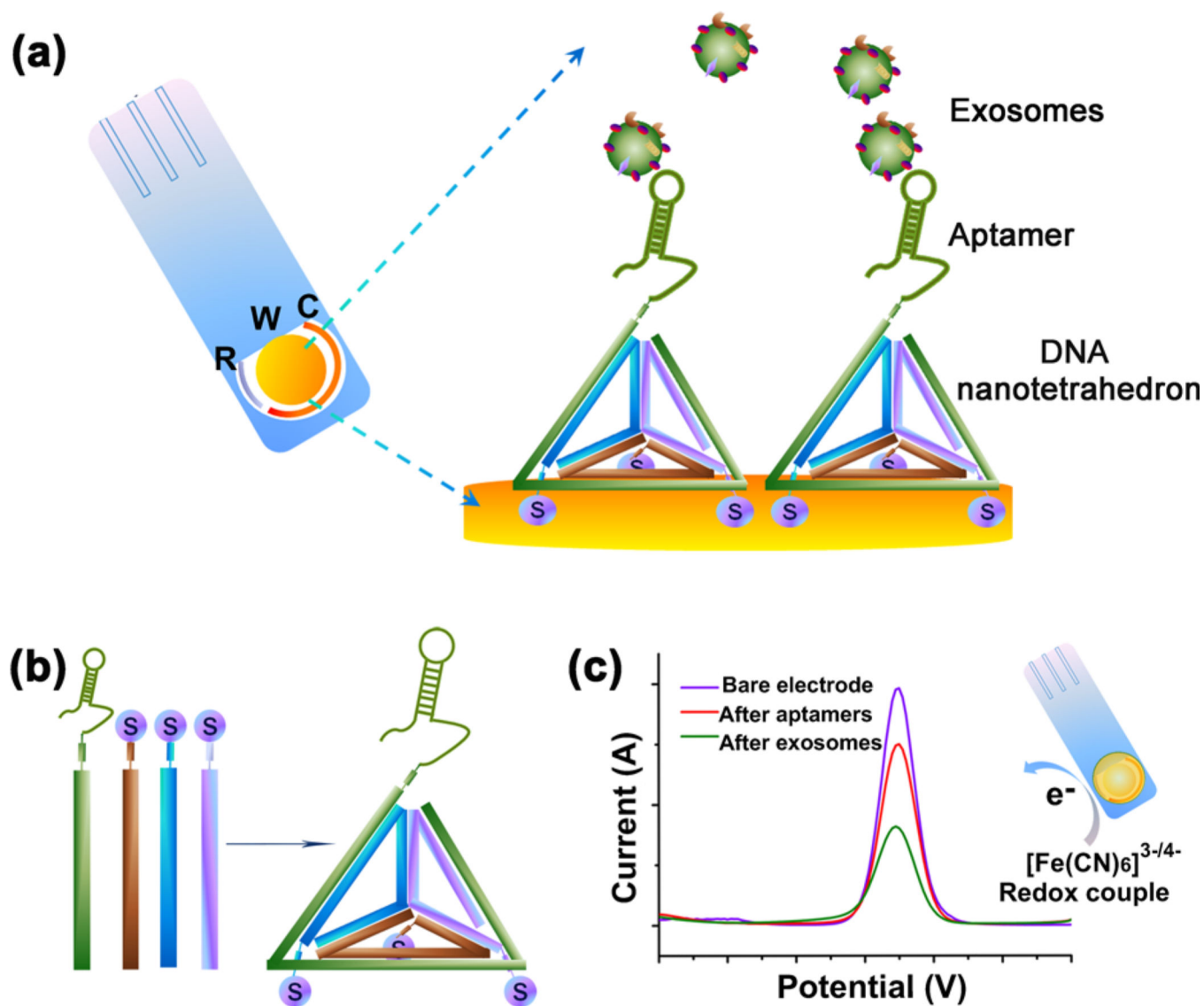


**Figure 3.** Self-assembly of aptamer-incorporated NTHs and electrochemical detection of hepatocellular exosomes with an NTH-assisted aptasensor. (a) Agarose gel electrophoretic analysis of the gradual formation of NTHs. DNA marker (lane M); sequence THa only (lane 1); dimer of THa and THb (lane 2); trimer of THa, THb, and THc (lane 3); NTH formed by THa, THb, THc, and Thd1 (lane 4). (b) Electrochemical current collection of a single-stranded aptamer-assisted and NTH-assisted aptasensor for detection of  $10^{13}$  hepatocellular exosomes per milliliter and data processing of electrochemical current signal before and

after aptamer capture of exosomes for each electrode. The relative suppression is given by

$\left(\frac{a-b}{a}\right) \times 100\%$ . (c) Concentration-dependent signal suppression of single-stranded aptamer-assisted and NTH-assisted aptasensors. The concentration of HepG2 exosomes varied from  $10^4$  to  $10^{13}$ /mL. Points were fitted using a log/logistic model. (d) Specificity analysis of the NTH-assisted aptasensor for detection of hepatocellular exosomes. The concentration of exosomes varied from  $10^4$  to  $10^{11}$ /mL. Points were fitted using a log/logistic model. (e) Calibration curve of the single-stranded aptamer-assisted aptasensor. The linear range of exosome concentration varied from  $10^6$  to  $10^{10}$  exosomes/mL. (f) Calibration curve of the NTH-assisted aptasensor. The linear range of exosome concentration varied from  $10^5$  to  $10^{12}$  exosomes/mL. All measurements were performed in triplicate, and the resulting data are displayed as average  $\pm$  SD.





### Scheme 1.

Schematic illustration of the NTH-assisted electrochemical aptasensor. (a) Aptamer-containing NTHs were immobilized *via* three thiol groups onto the gold electrodes for direct capture of exosomes in suspension. R: reference electrode area; W: working electrode area, with a diameter of 4 mm; C: counter electrode area. (b) Facile self-assembly of DNA nanotetrahedra from four single-stranded DNA sequences, which were mixed in equal concentrations, followed by heating at 95 °C for 2 min and “snap-cooling” at 4 °C for 1 min. (c) Redox signal changes after aptamer immobilization and after addition of exosomes. One drop of 5 mM  $\text{K}_3[\text{Fe}(\text{CN})_6]$ /100 mM KCl covered the entire electrode area for signal generation and amplification.